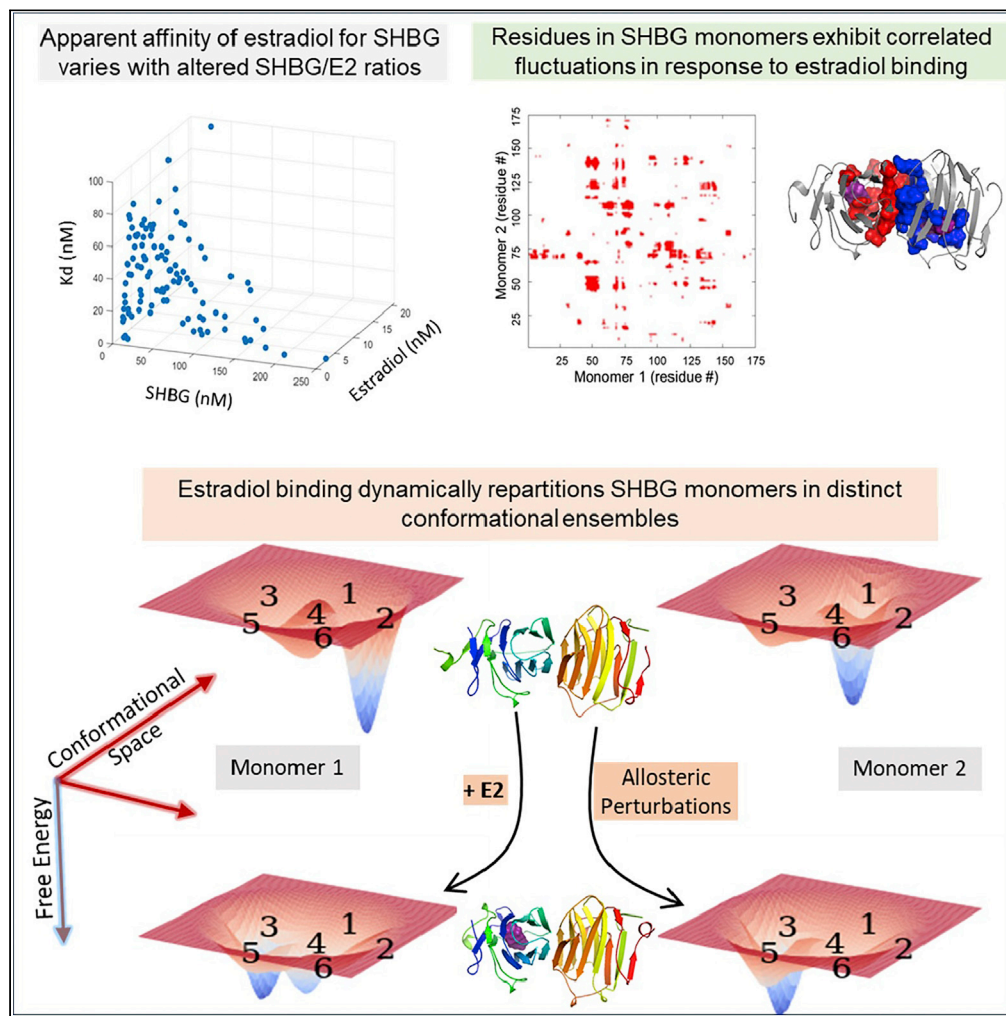


Article

Estradiol induces allosteric coupling and partitioning of sex-hormone-binding globulin monomers among conformational states



Ravi Jasuja, Daniel Spencer, Abhilash Jayaraj, ..., Kelly M. Thayer, David L. Beveridge, Shalender Bhasin

rjasuja@bwh.harvard.edu

Highlights

SHBG monomers exhibit conformational heterogeneity in free as well as bound states and are conformationally coupled

Estradiol's binding to SHBG is nonlinear and the "apparent" K_d changes with varying estradiol and SHBG concentrations

Estradiol's binding to each SHBG monomer differentially alters the conformational and energy landscapes of both monomers

Inter-monomeric allostery offers a versatile mechanism to extend the binding range of SHBG and regulate hormone bioavailability

Jasuja et al., iScience 24, 102414
June 25, 2021 © 2021 The Author(s).
<https://doi.org/10.1016/j.isci.2021.102414>

Article

Estradiol induces allosteric coupling and partitioning of sex-hormone-binding globulin monomers among conformational states

Ravi Jasuja,^{1,3,6,*} Daniel Spencer,¹ Abhilash Jayaraj,^{4,5} Liming Peng,¹ Meenakshi Krishna,¹ Brian Lawney,^{2,3} Priyank Patel,¹ Bhyravabhotla Jayaram,⁴ Kelly M. Thayer,⁵ David L. Beveridge,⁵ and Shalender Bhasin¹

SUMMARY

Sex-hormone-binding globulin (SHBG) regulates the transport and bioavailability of estradiol. The dynamics of estradiol's binding to SHBG are incompletely understood, although it is believed that estradiol binds to each monomer of SHBG dimer with identical affinity ($K_d \sim 2$ nM). Contrary to the prevalent view, we show that estradiol's binding to SHBG is nonlinear, and the "apparent" K_d changes with varying estradiol and SHBG concentrations. Estradiol's binding to each SHBG monomer influences residues in the ligand-binding pocket of both monomers and differentially alters the conformational and energy landscapes of both monomers. Monomers are not energetically or conformationally equivalent even in fully bound state.

Estradiol's binding to SHBG involves bidirectional, inter-monomeric allostery that changes the distribution of both monomers among various energy and conformational states. Inter-monomeric allostery offers a mechanism to extend the binding range of SHBG and regulate hormone bioavailability as estradiol concentrations vary widely during life.

INTRODUCTION

As living organisms became multicellular and more complex, hormones and circulating systems evolved to enable communication among distantly located cells and organs. The circulating binding proteins facilitated the transport of hormones and nutrients to various target tissues in the body. In humans and most mammalian species, most hormones are transported in the circulation, bound to their cognate binding proteins, and their bioavailability to the target tissues and their biological activity is regulated by the circulating concentration of the non-protein-bound fraction or the "free" hormone. The concept of the important role of binding proteins in regulating the bioavailability and biological activity of their ligands applies also to nutrients, such as vitamin D and B12, and many commonly used drugs, such as aspirin, warfarin, and some antibiotics.

Despite widespread adoption of the free hormone hypothesis, the dynamics of how hormones bind to their cognate-binding proteins have remained incompletely understood. Among the various physiologic ligands, the binding of sex hormones, estradiol and testosterone, to their high-affinity binding partner, sex-hormone-binding globulin (SHBG), remains the most extensively studied. Estradiol (E2), the dominant estrogen in men and women, is found in human circulation bound primarily to SHBG and human serum albumin (HSA) [Anderson, 1974; Dunn et al., 1981; Moll et al., 1981; Tietz, 1986; Peters, 1996; Pearlman et al., 1969; Burke and Anderson, 1972; Vigersky et al., 1979]. These circulating binding proteins regulate the transport, bioavailability, and metabolism of estradiol [Goldman et al., 2017; Rosner and Smith, 1975; Manni et al., 1985; Nisula and Dunn, 1979; Murphy, 1968; Zeginiadou et al., 1997; Laurent et al., 2016; Laurent and Vanderschueren, 2014]. Using an SHBG transgenic mouse model, Laurent et al. demonstrated that SHBG regulates the physiological function and the circulating half-life of sex steroids *in vivo*.

The dynamics of estradiol's binding to SHBG remain incompletely understood. It is generally believed that estradiol binds with high affinity to a single binding pocket in each of the two monomers of the SHBG dimer [Grishkovskaya et al., 2000; Grishkovskaya et al., 1999; Avvakumov et al., 2001], and prior studies have reported a single K_d (~ 2 nM) for each monomer [Dunn et al., 1981; Moll et al., 1981; Burke and Anderson,

¹Research Program in Men's Health: Aging and Metabolism, Boston Claude D. Pepper Older Americans Independence Center, Brigham and Women's Hospital, Harvard Medical School, Boston, MA, USA

²Center for Cancer Computational Biology, Dana-Farber Cancer Institute, Harvard Medical School, Boston, MA, USA

³Function Promoting Therapies, Waltham, MA, USA

⁴Supercomputing Facility for Bioinformatics and Computational Biology, Indian Institute of Technology, New Delhi, 110 016 India

⁵Departments of Chemistry, Molecular Biology, and Biochemistry and Molecular Biophysics Program, Wesleyan University, Middletown, CT, USA

⁶Lead contact

*Correspondence: rjasuja@bwh.harvard.edu
<https://doi.org/10.1016/j.isci.2021.102414>



1972; Avvakumov et al., 2001; Södergard et al., 1982; Vermeulen et al., 1999; Grishkovskaya et al., 2002; Mazer, 2009]. Underlying these studies, however, is the assumption that estradiol's binding to SHBG is linear and follows a one-to-one stoichiometry with identical affinity for both monomers.

Although the earlier studies assumed that there was an estradiol-binding pocket at the interface of the SHBG dimer [Sui et al., 1996], subsequent resolution of the crystal structure of the N-terminal recombinant human SHBG containing the ligand-binding pocket (LBP) complexed with steroidal ligands [Grishkovskaya et al., 2000; Grishkovskaya et al., 1999; Avvakumov et al., 2001] revealed a homo-dimeric structure in which each monomer contains an LBP for estradiol. Observations that dimerization-deficient SHBG variants bound estradiol with an affinity similar to that of wild-type SHBG [Avvakumov et al., 2001; Petra et al., 2001] led to the now common view that the binding of estradiol to each monomer is equivalent and independent of its binding to the second monomer. Since then, the linear binding model with a K_d of ~ 2 nM for each monomer has remained the prevalent dogma in the literature.

Several published observations are inconsistent with the prevalent notion of linear binding of estradiol to SHBG in which both binding sites on the SHBG dimer are equivalent in their binding affinity. First, only a narrow range of estradiol concentrations were used in the binding data, which were fit to linear Scatchard plots to derive a single K_d [Dunn et al., 1981; Moll et al., 1981; Burke and Anderson, 1972; Södergard et al., 1982]. The linear transformation of data over a limited range of hormone concentrations may have prevented a complete understanding of estradiol association dynamics. Second, widely varying binding affinities have been reported for estradiol binding, ranging from as low as picomolar [Wu et al., 1976] to as high as 25 nM [Sui et al., 1996], depending on the estradiol and SHBG concentrations. These findings suggest that the apparent K_d might be affected by the estradiol concentrations and the estradiol to SHBG ratio, which would only be possible if there were a concentration-dependent allosteric interaction between the two binding sites on the SHBG dimer. Third, even in the presence of super-saturating estradiol concentrations, the crystal structure of the second monomer within the SHBG dimer could not be resolved. One possible explanation for the failure to resolve the crystal structure of the second monomer is that the two monomers are not equivalent in their conformations and energy states even though they have the same amino acid sequence [Grishkovskaya et al., 1999].

Although the estimates of estradiol's binding affinity to SHBG have varied among studies, it is generally believed that its affinity is slightly lower than that of testosterone [Dunn et al., 1981; Moll et al., 1981; Burke and Anderson, 1972; Södergard et al., 1982; Orwoll et al., 2006]. If these estimates of the relative binding affinities of estradiol and testosterone are correct, and if both bind to the same pocket in SHBG, then, given the much higher serum concentration of testosterone than estradiol in men ($5000\text{--}6000\text{ pg}\cdot\text{mL}^{-1}$ for testosterone versus $20\text{--}50\text{ pg}\cdot\text{mL}^{-1}$ for estradiol), substantially less estradiol should be bound to SHBG under physiological conditions than what is observed [Dunn et al., 1981; Burke and Anderson, 1972; Södergard et al., 1982]. Thus, it is difficult to reconcile these data with the notion of linear binding kinetics and a single K_d of ~ 2 nM.

To gain a better understanding of the binding dynamics of this system, we employed multiple biophysical techniques, modern computational tools, and Markov state modeling to examine nonlinear data derived from the binding isotherms and depletion curves. Some of the original studies were limited by the varying dialysis conditions, failure to account for protium-tritium exchange when using tritium-labeled tracers, and the inclusion of a narrow range of estradiol and SHBG concentrations. As described in the [transparent methods](#) section, we took several steps to overcome these methodological concerns and to minimize their influence. Our studies provide evidence of a nonlinear, dynamic binding process involving allosteric coupling between the SHBG monomers that changes the energy landscape of both monomers and their distribution between various energy states such that the two monomers are not equivalent, even in the fully bound state, and offer functional insight into the ligand-induced, inter-monomeric interactions and conformational heterogeneity in SHBG.

RESULTS

Estradiol binding to SHBG exhibits complex interaction dynamics

Equilibrium dialysis experiments were performed using a wide range of SHBG concentrations at varying estradiol to SHBG ratios, and the resulting isotherms for estradiol's binding to SHBG are shown in [Figure 1A](#). The bound and free estradiol fractions were determined by measuring the estradiol concentrations

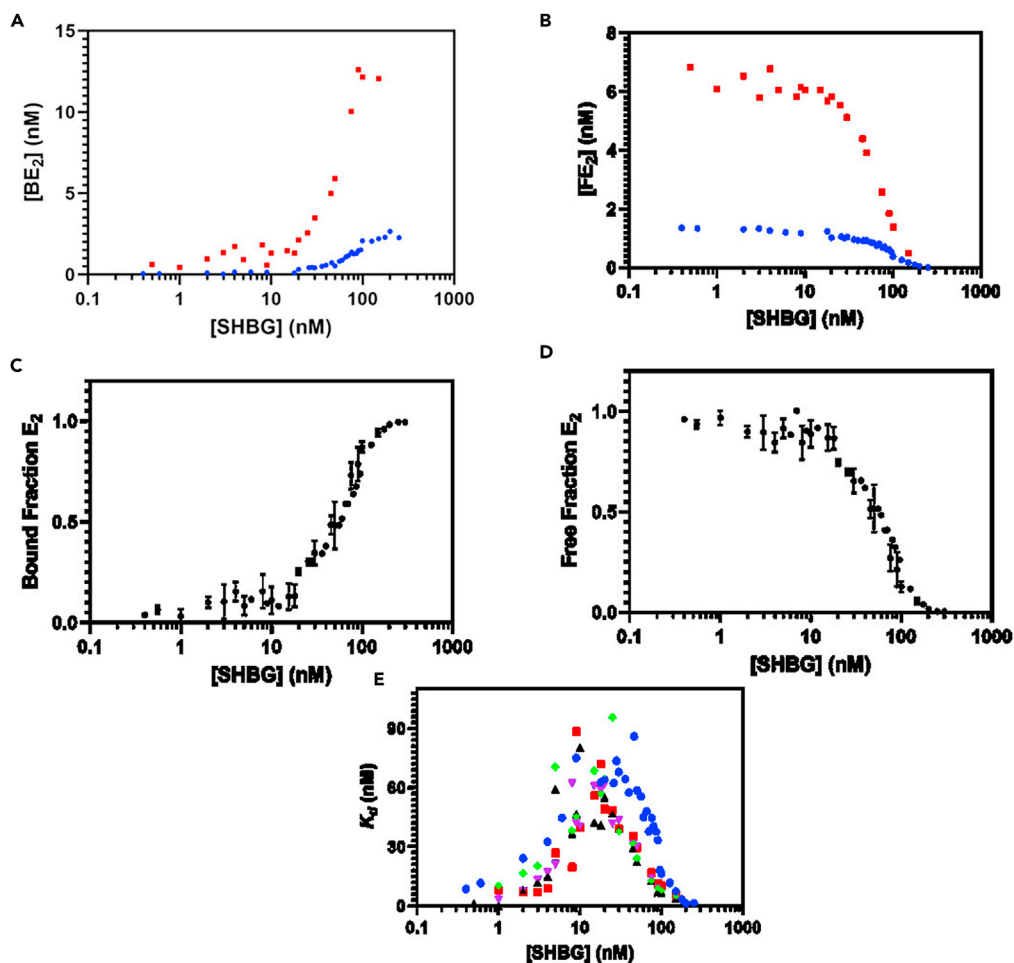


Figure 1. The equilibrium dialysis experiments demonstrate that estradiol binding to the SHBG dimer is a dynamic, nonlinear process

(A) The binding isotherm, generated by the titration of increasing SHBG concentrations in the presence of a fixed estradiol concentration (either 2.6 or 13.7 nM). The data from representative experiments conducted at the respective estradiol concentrations of either 2.6 nM (blue circles) or 13.7 nM (red squares) are shown. The binding isotherm shows nonlinearity of binding as well as asymmetry around the 50% [BE₂] point, which is inconsistent with the prevalent notion of linear binding with a single dissociation constant, K_d .

(B) The corresponding depletion curve, generated by plotting the concentration of the free estradiol that was dialyzed into the buffer side of dialysis chamber against the SHBG concentration.

(C) The fraction of estradiol that was bound to SHBG ($[bound\ E2]/[total\ E2]$) on the sample side of the dialysis chambers at each SHBG concentration. Each data point represents the average E2 and SHBG concentration from two experiments.

(D) The fraction of estradiol that was free ($[free\ E2]/[total\ E2]$) at each SHBG concentration. Each data point represents the average of free E2 and SHBG concentration from two experiments.

(E) A plot of the apparent K_d versus the SHBG concentration in the equilibrium dialysis experiments performed at five E2 concentrations: 2.6 nM (blue circles), 3.8 nM (green diamonds), 4.1 nM (black triangles), 7.1 nM (purple inverted triangles), and 13.7 nM (red squares). At each SHBG concentration, the apparent K_d was determined from the measured SHBG and the measured free and bound estradiol concentrations. The apparent K_d varied non-linearly as the SHBG concentrations and SHBG:E2 ratios were varied.

on each side of the dialysis membrane using LC-MS/MS after overnight incubation (transparent methods). As the SHBG concentration increased, an increasing amount of estradiol partitioned into the sample side. Figure 1B shows the corresponding depletion curves, which were generated by plotting the decreasing free estradiol concentrations on the buffer side of the dialysis membrane, as the SHBG concentration was increased. The binding and depletion curves generated by plotting the fraction of bound and free estradiol from two independent experiments are shown in Figures 1C and 1D.

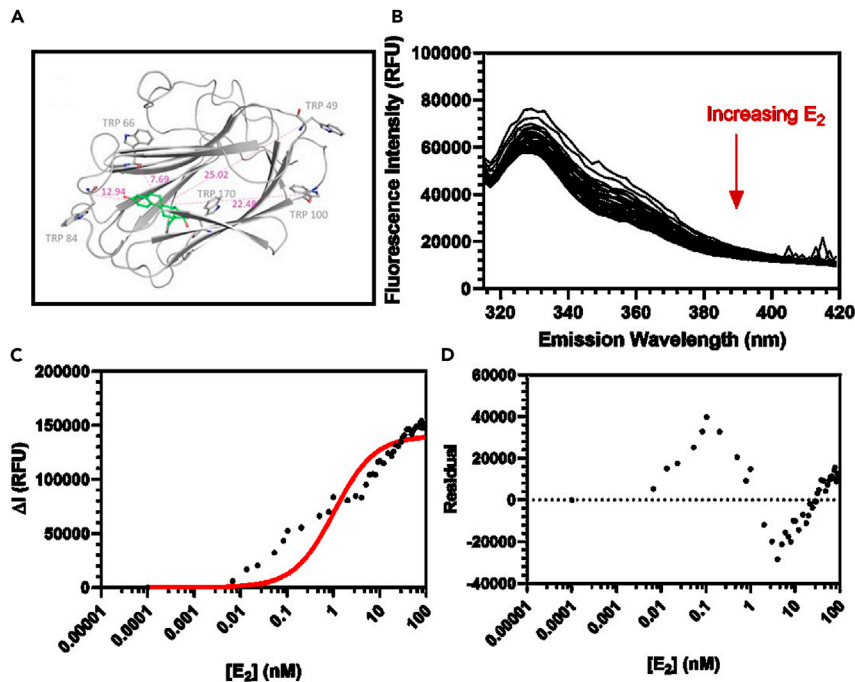


Figure 2. Estradiol binding to SHBG alters the microenvironment of tryptophan residues and quenches the fluorescence emission intensity

(A) The relative distance of tryptophan residues from the estradiol ligand in the binding pocket. The residue coordinates were obtained from the crystal structure (PDB ID: 1LHU). The distances between the alpha carbons are mapped for the five tryptophan residues in SHBG to the C₉ position on E₂.

(B) The steady state emission spectrum from tryptophan residues as the estradiol concentration was increased from subphysiologic (0.0001 nM) to supraphysiologic (100 nM) range. The data were collected with 1-mm slit width using λ_{ex} of 290 nm, and emission was collected from 310 nm to 410 nm.

(C) A plot of the changes in integrated emission from tryptophan residues in 20 nM SHBG at increasing estradiol concentration. The binding curve predicted by the extant, linear model of SHBG:E₂ association assuming homogeneous interaction with both monomers with a fixed K_d of 2 nM (solid red curve) does not fit the experimental binding data, shown in solid black symbols.

(D) Plots of the residuals between the predicted (red curve in Figure 2C) and experimentally measured data points at graded E₂ concentrations and shows that the prevailing linear binding model exhibits under- and overestimation from the experimentally derived binding curve at various E₂ concentrations.

The binding isotherm generated using equilibrium dialysis was not symmetric around the point corresponding to 50% bound estradiol; the complex asymmetry of the binding isotherm is inconsistent with the notion of homogeneous binding of estradiol to SHBG with a single K_d (Figure 1). From experimentally derived bound and free estradiol concentrations at each SHBG concentration, the apparent K_d was computed at various estradiol concentrations (Figure 1E). The apparent K_d varied with the SHBG concentration and the relative ratio of estradiol and SHBG concentrations, inconsistent with the prevailing model of homogeneous binding of estradiol to SHBG with a single K_d . The variation in apparent K_d at varying concentrations of estradiol and SHBG indicates that there are multiple equilibria in the estradiol-SHBG interaction with distinct affinities. These data do not support the view that the two monomers have equivalent binding affinity for estradiol. The binding isotherms in Figure 1A are also inconsistent with two static K_d values, one for each monomer. These data raise the possibility that the binding sites on the two monomers are allosterically coupled to enable dynamic changes in the apparent K_d that is influenced by the relative concentrations of estradiol and SHBG.

Intrinsic tryptophan emission from SHBG provides evidence that estradiol binding is multiphasic and associated with changes in tryptophan micro-environment

Of the 11 tryptophan residues in the full-length SHBG, the LG domain possesses five tryptophan residues, two of which (W66 and W170) are near the LBP (Figure 2A). Accordingly, we utilized the perturbations in the

emission from the tryptophan residues to monitor estradiol's binding to SHBG at graded estradiol concentrations.

Figure 2B shows the emission spectra of 20 nM SHBG titrated with a wide range of estradiol concentrations that extended from the subphysiologic to supraphysiologic range. The system was excited at 290 nm, and the emission spectrum was collected from 314 to 420 nm. As increasing concentrations of estradiol were titrated into the SHBG solution, we observed a significant concentration-dependent reduction in intrinsic tryptophan emission. The concentration-dependent increase in quenching of tryptophan fluorescence from SHBG solution suggests that estradiol binding is associated with changes in the tryptophan micro-environment due to conformational rearrangement in SHBG.

In addition to monitoring the perturbations in the fluorescence spectra, integrated emission intensity from tryptophan was independently collected through a long-pass filter (WG305). The emission spectra presented in Figure 2B were used to generate the binding isotherm shown in Figure 2C. The observed binding isotherm shows that estradiol binding to SHBG is a nonlinear process that does not conform to the isotherm predicted by a linear binding model that assumes a single K_d (the red curve in Figure 2C). The binding isotherm predicted by the linear binding model with a single K_d (red curve) underestimates estradiol binding in the lower concentration range and overestimates binding in the higher concentration range, as shown in the residual plot (Figure 2D). The binding isotherms generated from intrinsic tryptophan fluorescence quenching independently corroborate the presence of multiple binding equilibria observed previously in the dialysis data presented in Figure 1.

Estradiol-induced molecular rearrangement alters the conformational states of residues in the ligand-binding pockets of SHBG monomers, suggesting inter-monomeric allosteric coupling

We performed molecular modeling studies to evaluate whether estradiol binding to SHBG induces conformational rearrangements in the estradiol-binding pocket and in regions distant from the binding pocket. Protein backbone flexibility computations are an important tool to examine the alterations in the equilibrium distribution of protein conformations. The intrinsic conformational flexibility parameters have been recognized as contributors to protein function and are calculated by relaxing the atomic environment starting from the static crystal structure and provide complementary characterization of the conformational perturbations in the estradiol-bound states of SHBG. The estradiol-bound SHBG crystal structure was used to probe the contacts that estradiol makes with the amino acids in the binding pocket and the dimerization interface. We performed trajectory analysis of the observed alterations in the flexibility of the protein backbone in three populations of SHBG molecules: (1) the unliganded SHBG dimer (SHBG:0 $\times 10^2$); (2) the singly bound state in which only the ligand-binding pocket of the first monomer is occupied (SHBG:1 $\times 10^2$), and (3) the fully bound state in which both monomers are bound with estradiol (SHBG:2 $\times 10^2$). The structures were allowed to minimize and equilibrate using the AMBER suite for molecular dynamics simulations (ff14SB forcefield, 10 Å cutoff), and trajectories were monitored over 5 μ s. The dynamics of the residue rearrangement calculated for the unliganded SHBG and the estradiol-bound forms of SHBG with one or both of the LBPs occupied are reflected in the RMSD plots.

To examine the allosteric coupling between the two SHBG monomers, the LBPs of each monomer (Figures 3A–3C) were followed as SHBG progressed from unliganded (SHBG:0 $\times 10^2$) to singly bound (SHBG:1 $\times 10^2$) to doubly bound (SHBG:2 $\times 10^2$) states. Figure 3A shows that even in the unliganded SHBG dimer, the ligand-binding pockets in the two monomers populate distinct conformational states. As expected, the conformational flexibility of the LBP of monomer 1 was altered upon the binding of estradiol to monomer 1 (Figure 3B, blue trace). Similarly, the conformational states of the LBP of monomer 2 are sensitive to the binding of estradiol to the first monomer as evidenced by the altered trajectories of these residues in the singly bound state (Figure 3B, red trace). Even more interestingly, the binding of the second estradiol molecule to monomer 2 altered the conformational states in the LBP of monomer 1, which was already occupied by estradiol (Figure 3C, blue trace).

Time-resolved lifetime fluorescence spectroscopy using bis-ANS demonstrates that estradiol binding significantly alters the global conformational state of the SHBG:E2 complex

The data from the equilibrium dialysis, steady-state fluorescence emission experiments, and molecular modeling studies suggested that estradiol binding sites on the two SHBG monomers are allosterically

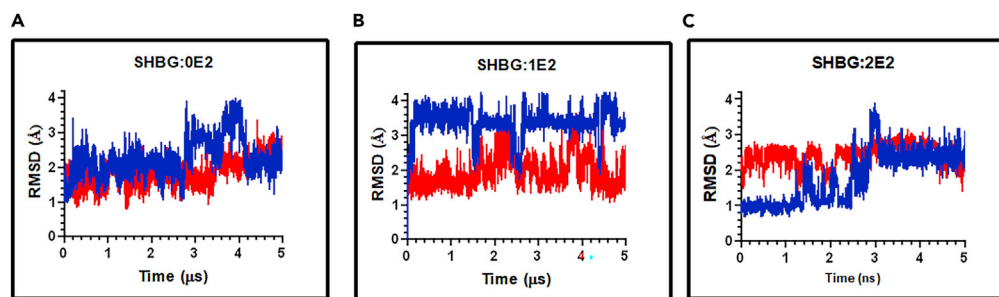


Figure 3. Trajectories of residues within the ligand-binding pockets (LBP1 and LBP2, respectively) of the first and second monomer show conformational coupling between the two SHBG monomers

The plots depict the temporal evolution of trajectories over 5 μ s of the three structures: SHBG:0 \times 10²—unliganded SHBG dimer (3A); SHBG:1 \times 10²—singly bound state in which only the first monomer is bound to estradiol (3B); and SHBG:2 \times 10²—doubly bound state in which the second monomer also is occupied by estradiol (3C).

Blue color represents monomer 1 (LBP1); red color represents monomer 2 (LBP2). A comparison of the trajectories in (3A) and (3B) shows that the binding of estradiol to the LBP of the first monomer changes the population of conformational states not only in monomer 1 but also in monomer 2, providing evidence of the allosteric interaction between the monomers.

(3C) The subsequent binding of the second estradiol to the LBP of the second monomer in the doubly bound state alters the conformational state of the LBP of the second monomer but also of the first previously occupied LBP of the first monomer, providing further evidence of the bidirectional inter-monomeric allostery.

coupled: the ligand binding to one of the SHBG monomers induces conformational rearrangement that is associated with alterations in the conformation of the second binding site in the SHBG dimer. We sought additional validation of these findings by examining the partitioning of a hydrophobic fluorescent probe, 4,4'-dianilino-1,1'-binaphthyl-5,5'-disulfonic acid (bis-ANS), into the interior of SHBG. bis-ANS has been used extensively as a sensitive probe to interrogate the steady state and kinetics of ligand-induced conformational changes in receptor proteins. Accordingly, we measured changes in the solvent accessible surface area and global conformational changes in the SHBG protein as graded concentrations of estradiol were added to a solution containing bis-ANS and SHBG.

In the absence of SHBG, bis-ANS was efficiently quenched in the aqueous environment, with a singlet-excited state lifetime of approximately 250 ps and low quantum yield. Once partitioned in the interior of a protein, bis-ANS molecules display longer lifetimes in the range of 5–8 ns with concomitant increase in fluorescence emission. The excited state emission data fit to two decays (Figure 4) corresponding to 1.2 ns and 6.7 ns with χ^2 between 1 and 2.3. The fractional intensities of the short- and long-lifetime components were found to be sensitive to estradiol concentrations reflecting the estradiol-induced global conformational rearrangement and repartitioning of bis-ANS within the SHBG dimer upon ligand binding.

Figure 4A shows the phase and frequency modulation data as graded concentrations of estradiol were added to a solution containing SHBG and bis-ANS. The titration of estradiol into an SHBG solution led to concentration-dependent changes in bis-ANS partitioning. Alterations in integrated fluorescence from bis-ANS could result either from repartitioning of the hydrophobic probe in the protein interior or from changes in fluorescence lifetimes. Accordingly, we analyzed the phase and frequency modulation data to determine the fractional contributions of free and bound bis-ANS and the singlet excited state lifetimes. Estradiol titration into SHBG exerted only a minimal effect on the excited state lifetimes of the bound and free bis-ANS (Figures 4B and 4C). However, as the estradiol concentration was increased, the fractional contribution from the short-lifetime component substantially increased and that of the long-lifetime component decreased (Figures 4D and 4E), indicating that estradiol binding to SHBG leads to global conformational changes in SHBG, stabilizing overall structure and expelling bis-ANS from the protein interior.

Dynamic cross-correlation matrix analysis shows allosteric changes in residue correlations upon estradiol binding to either of the two monomers

To analyze the effect of the estradiol binding on the residue rearrangement in each of the two monomers in the three states (unliganded, Figure 5A; singly bound, Figure 5B and doubly bound, Figure 5C), dynamic

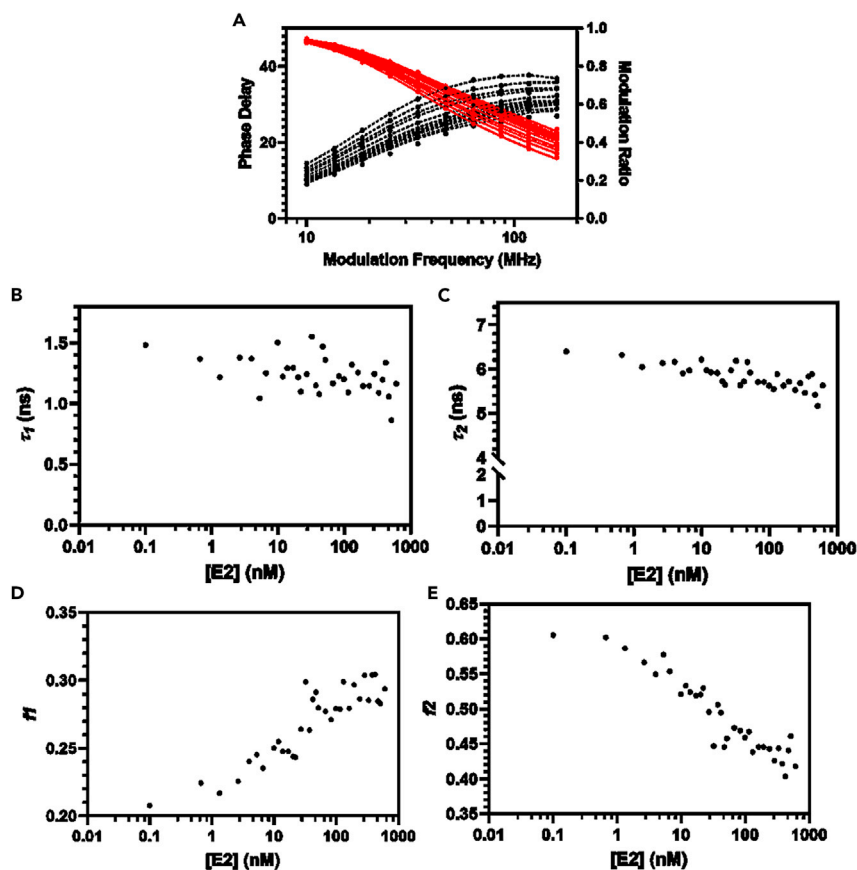


Figure 4. Time-resolved lifetime fluorescence spectroscopy using an extrinsic fluorescent probe, bis-ANS, demonstrates that estradiol binding significantly alters the global conformational state of the SHBG:E2 complex (A) The raw data and fits to the phase delay and modulation ratio obtained at increasing estradiol concentrations titrated into a solution of 40 nM SHBG and 500 nM bis-ANS. The modulation frequencies were altered from 10 to 160 MHz to determine τ_{phase} and τ_{mod} at each SHBG:E2 ratio. The excited state lifetime data were satisfactorily fit to the most parsimonious model of two emitting species where the chi square values ranged from 0.8 to 2.1. (B) and (C) The short and long lifetime components, respectively, as a function of estradiol concentrations. (D) and (E) The change in fractional (f_1 and f_2) and fluorescence contribution from the bis-ANS populations exhibiting short and long singlet excited state lifetime components. Collectively, the data indicate that estradiol binding to SHBG induces global conformational change in the protein as evidenced by the significant change in relative populations of bis-ANS species exhibiting the long and short singlet excited state lifetimes.

cross-correlation matrices (DCCM) were generated for each residue in the two monomers. The right panels for each of the DCCM plots show the spatial location of residues, which exhibit correlated motions at the dimerization interface and in the LBPs across two monomers in each of the states. Contrary to what would be predicted by the prevailing linear model of estradiol binding to SHBG, DCCM plots show that residue correlations in monomers within the unliganded dimer are not identical and that each monomer samples distinct conformational states even in the absence of estradiol. The binding of the first estradiol molecule to monomer 1 resulted in changes in correlated motions in residues of both monomers 1 and 2 (Figure 5B). Similarly, the binding of estradiol to monomer 2 resulted in substantial changes in the coupling of motions in the residues of estradiol-bound monomer 1 (Figure 5C). Collectively, the occurrence of several new correlations within each monomer when estradiol binds to either of the two monomers provides evidence of an allosterically coupled network of residues within the two monomers of SHBG.

Markov state models reveal dynamic allosteric conformational coupling between the SHBG monomers

Markov state models have been used to study the protein conformational transitions in ligand-bound and unbound states and to estimate the state composition from population-averaged residue trajectory data

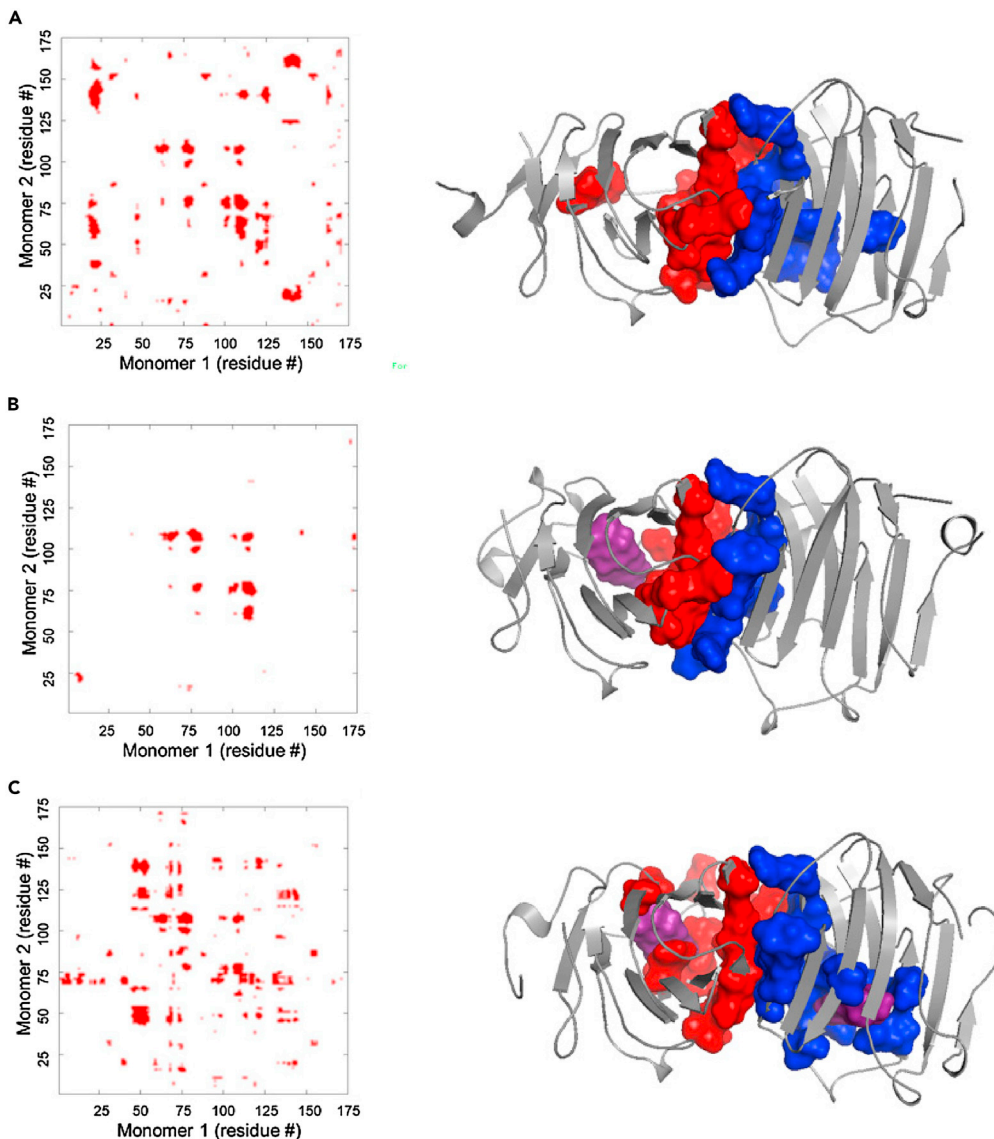


Figure 5. Dynamic cross-correlation matrices for SHBG dimer illustrate that distant residues in the two monomers are conformationally coupled and respond to binding of estradiol to either of the two monomers

Inter-monomeric residue motion correlations were examined for the three states: unliganded (5A; SHBG:0 $\times 10^2$), singly bound (5B; SHBG:1 $\times 10^2$), and doubly bound (5C; SHBG:2 $\times 10^2$). The quadrants depicting the inter-monomer correlation show changes in coordinated movement of the residues in the two monomers. Red color intensity stands for strength of residue correlation. The correlated motions whose absolute values were smaller than 0.3 were not included. The right panels show the location of distant residues at the inter-monomeric interface and ligand-binding pockets in the two monomers that are conformationally coupled in the respective liganded states. Only the residues, which show correlated movement, are colored in monomer 1 (red) and monomer 2 (blue). Estradiol molecule is represented in purple color. Collectively, these data show that allosteric coupling in binding estradiol is manifested through coordinated dynamic rearrangement of residues in each of the two SHBG monomers.

[Shukla et al., 2015; Chodera and Noe, 2014; Schwantes et al., 2014; Prinz et al., 2011; Thayer et al., 2017]. We utilized the Markovian framework to examine all-atom molecular modeling trajectories and determined the estradiol-induced redistribution of SHBG monomers among various conformational ensembles and their temporal distribution in microstates after estradiol binding. Inter-monomeric allostery within the SHBG dimer was studied using the AMBER suite of programs to generate conformational clusters based on pairwise RMSD measures using a k-means algorithm. Spanning the project space for the possibility

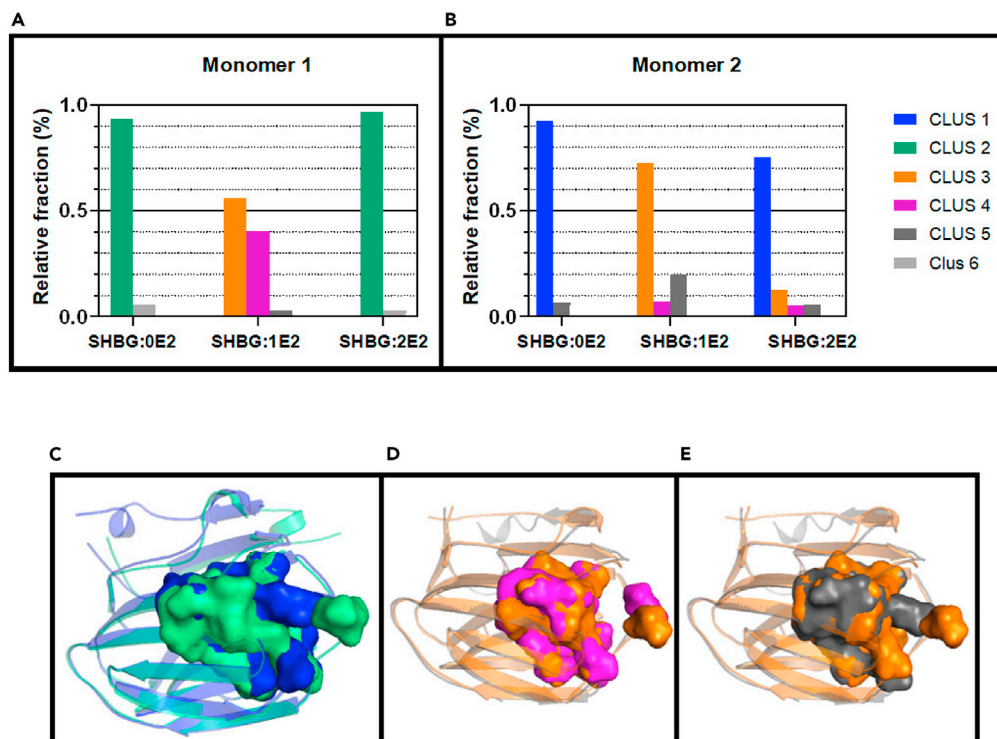


Figure 6. The two monomers within the SHBG dimer populate distinct conformational clusters, which change dynamically upon ligand binding

Relative frequency distribution of SHBG conformational states occupied by each of the monomers (6A, monomer 1; 6B monomer 2) in response to the binding of the first and the second estradiol molecule to SHBG dimer. The most parsimonious Markov State modeling analysis shows that six conformational states are involved in this dynamics as depicted in this histogram of the distribution of the two monomers in various conformational clusters in the unliganded, singly bound, and doubly bound SHBG. Inset displays the color corresponding to the conformational clusters that each SHBG monomer occupies in the unbound and bound states.

As shown in the (6A), (6B), and (6C), the monomers dynamically repartition predominantly in clusters 1–5 as the SHBG dimer transitions between unliganded, singly bound, and doubly bound states. We posit that this multi-state conformational equilibria manifests as apparent K_d being sensitive to the SHBG/E2 ratio. For this to be true, one would expect that the conformational arrangement of residues in the ligand-binding pockets in these conformational clusters would be distinct. There we generated pairwise overlays for the clusters occupied in the monomers in unbound, singly and doubly bound SHBG dimer.

(6C), (6D), and (6E) The spatial distinction in the orientation of ligand-binding pocket residues in the various clusters.

Figure 6C shows the overlay of LBP residues in clusters 1 (blue) and 2 (green). Figures 6D and 6E illustrate the changes in LBP residues in clusters 3 (orange), 4 (cyan), and 5 (gray), which are predominantly occupied by monomers 1 and 2 in the singly bound states of SHBG dimer.

The color coding of the residues in (6D), (6E), and (6F) corresponds to the cluster population colors in histograms in Figures 6A–6C, respectively.

of 2–12 clusters, the most parsimonious distribution of clusters was found to be 6 (Figure 6, clusters C1–C6). Distribution functions of the distances of the SHBG microstates with respect to each cluster centroid were calculated for the six clusters.

Figure 6 shows that the two monomers populate the six conformational clusters to varying degrees depending on the estradiol occupancy. Even in the unliganded state, the monomers populate conformationally distinct clusters and are not equivalent (Figures 6A–6C). When neither of the two monomers is occupied by the ligand, monomer 1 is distributed predominantly between conformational clusters C2 and C6, but monomer 2 is distributed predominantly in clusters C1 and C5 (Figures 6A and 6B; SHBG:0 × 10²). Notably, binding of the first estradiol molecule not only alters the conformational ensemble of monomer 1 but also changes the distribution of monomer 2 in clusters C3, C4, and C5, providing evidence of inter-monomeric

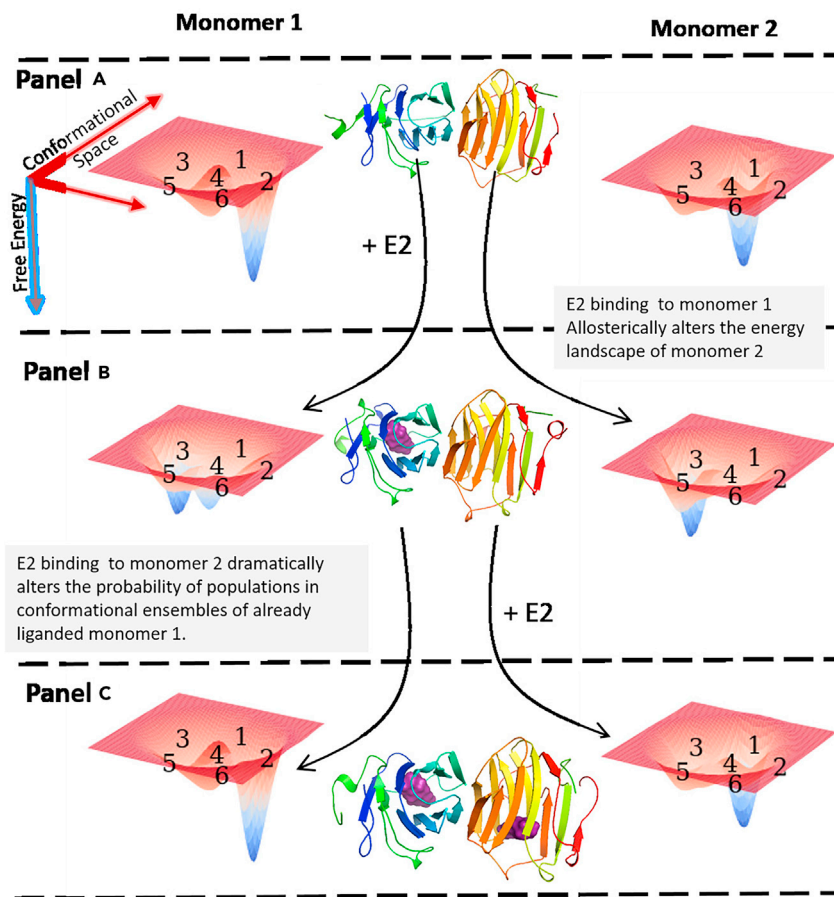


Figure 7. Estradiol binding to either of the two monomers alters the conformational energy landscape of the other monomer

The three panels collectively show the ensemble allosteric modulation of relative probabilities of population of clusters and respective transition rates between the conformational substates in response to estradiol binding to monomers.

(A) The two unliganded SHBG monomers populate distinct conformational states.

(B) Upon estradiol binding to monomer 1, not only are the conformational states of monomer 1 impacted but the monomer 2 also is allosterically affected.

(C) Illustration of estradiol binding to monomer 2 that alters the conformational states of the already bound monomer 1 such that even in the fully bound state, the monomers within the SHBG dimer are not equivalent and exhibit conformational heterogeneity.

allostery (Figures 6A and 6B; SHBG:1 $\times 10^2$). When the second estradiol molecule binds to monomer 2, it not only influences populations of conformational states of monomer 2 but also changes the distribution of the conformational states of the already occupied monomer 1 (Figures 6A and 6B; SHBG:2 $\times 10^2$).

To determine if the orientation of the binding pocket residues differed among the clusters, we generated the overlay of the cluster pairs (Figures 6C–6E), which were predominantly populated by the two monomers in the three states (SHBG:0 $\times 10^2$, SHBG:1 $\times 10^2$, and SHBG:2 $\times 10^2$). We find that the conformational states populated by the monomers in these clusters are substantially different both in the ligand-binding pockets and in the residues, distant from the ligand-binding pocket. The relative probability of partitioning of monomers in distinct conformational clusters and the associated transition rates were used to elucidate the energy landscapes for each monomer.

The Markov state model (MSM) analyses revealed that even in the absence of estradiol, the two monomers within the SHBG dimer exhibit distinct energy landscapes (Figure 7) and that estradiol binding is associated with dynamic redistribution of ensemble populations. Figure 7A shows that the unliganded SHBG

monomers occupy distinct energy landscapes consistent with their conformational heterogeneity in the unliganded state. Upon binding of estradiol to the first monomer, the populations of energy states occupied by each of the two monomers are altered (Figure 7B). The relative probabilities for occupancy of conformational clusters for both the monomers are sensitive to the occupancy of either of the two monomers (Figure 7B). Similarly, the energy landscape of the estradiol-bound first monomer is subsequently altered by estradiol's binding to the second monomer.

These data demonstrate that estradiol binding to either of the monomers alters the conformational states and energy landscapes of both monomers. The net effect of the perturbations associated with estradiol binding is the reshaping of the free-energy landscape of each monomer and stabilizing distinct conformational states. Such dynamic redistribution of SHBG conformational ensemble into clusters could explain the continuum of apparent affinity of estradiol for the SHBG dimer, depending on the relative concentrations of estradiol and SHBG, observed in the equilibrium dialysis and optical spectroscopy experiments.

DISCUSSION

We present here several lines of evidence, generated using multiple experimental approaches, that show that the prevalent linear model of estradiol's binding to SHBG, which posits homogeneous binding of estradiol with equivalent K_d values for the two binding sites on the SHBG dimer (one on each of its monomers), is inconsistent with experimental data. First, the binding isotherms of estradiol's association with SHBG generated using equilibrium dialysis and steady-state fluorescence spectroscopy are neither linear nor symmetric around the point corresponding to 50% bound estradiol concentration; the complex asymmetry of the binding isotherm is inconsistent with the notion of homogeneous binding of estradiol to SHBG with a single K_d . The binding isotherms also do not conform to two rigid binding sites, each with a fixed but distinct K_d . Second, the apparent K_d varied substantially as the concentrations of estradiol and SHBG as well as the ratios of their relative concentrations were varied. Because the primary amino acid structure of the two monomers within each SHBG dimer is identical, the dynamic concentration-dependent variation in the apparent K_d can only be explained by a dynamic intra-molecular conformational rearrangement within the SHBG dimer upon ligand binding that alters the K_d of the ligand binding pocket. Third, when we used bis-ANS probe to examine its partitioning into the interior of SHBG, we found that the fractional intensities of its short- and long-lifetime components were highly sensitive to estradiol concentrations. With increasing estradiol concentrations, the short-lifetime fraction increased, suggesting a more compact SHBG structure in the ligand-bound state. The estradiol-induced repartitioning of the bis-ANS probe within SHBG provides direct experimental evidence of a global conformational rearrangement in SHBG upon estradiol binding. Finally, the molecular modeling simulations reveal that estradiol binding to monomer 1 induces conformational rearrangements in the estradiol-binding pocket of both monomers. Thus, the molecular modeling studies provide support for the allosteric interaction between the two monomers upon ligand binding.

The variations in the apparent K_d with varying estradiol concentrations and estradiol to SHBG ratios and the heterogeneity in binding isotherms were also noted in some previous investigations of testosterone and dihydrotestosterone binding to SHBG [Heinrich-Balard et al., 2014; Zakharov et al., 2015; Metzger et al., 2003]. However, these divergences in the apparent K_d and the nonlinearities in the binding isotherms were ignored in favor of the simplistic homogeneous interaction model. Furthermore, a limited range of estradiol concentrations used in some studies may have prevented a complete understanding of the complex nonlinear binding dynamics observed over a wider range of estradiol and SHBG concentrations.

Markov state models developed using the molecular dynamics trajectories provide a detailed understanding of the molecular processes involved in the allosteric coupling between SHBG monomers. The conformational clustering analysis from states-and-rates network models illustrate that binding of the first estradiol molecule significantly alters the probabilities of the distribution of both monomers in various conformational states as well as the associated energy landscapes of both monomers. Interestingly, binding of the second estradiol molecule to monomer 2 also impacts the landscape and probability of conformational transitions in estradiol-bound monomer 1. The Markov state models show that allosteric coupling in the SHBG monomers changes the energy landscape such that the two monomers are not equivalent even in the fully bound state. The RMSD plots for the monomer 1 in the singly bound state and the

monomer 2 in the doubly bound state show that estradiol binding substantially perturbs the conformation of the monomer where it binds. The trajectory analysis combined with detailed cluster classification show that conformational landscape of monomer 1 in SHBG:1 $\times 10^2$ and monomer 2 in SHBG:2 $\times 10^2$ are substantially different. Collectively, these data suggest that the two ligand-binding events manifest heterogeneous conformational perturbations in the two monomers. Monomer 1 occupies similar conformational clusters in the unliganded and fully bound states, whereas the monomer 2 exhibits a completely distinct energy landscape. Detailed studies of on/off rates and structural characterization would be required to provide experimental support, but we posit that these data suggest an intriguing mechanistic insight. It appears that the estradiol preferentially binds to the first monomer, but it is the second monomer that preferentially releases the ligand because monomer 1 in the fully bound state reverts to the high-affinity state. This hysteresis in binding and release dynamics could significantly extend the dynamic range of the SHBG's functional capacity in regulating transport, bioavailability, and metabolism. Collectively, these studies provide comprehensive evidence of a non-linear, allosteric process where the association dynamics cannot be faithfully represented by a single bimolecular association constant.

The ligand-induced allosteric interaction between the monomers observed during estradiol's binding to SHBG may be a more general mechanism among multimeric binding proteins. We have previously found evidence of ensemble allostery in testosterone's binding to SHBG [Zakharov et al., 2015]. Our subsequent studies of testosterone's binding to human serum albumin revealed that testosterone can bind multiple (at least 6) binding sites on HSA and that testosterone binding to one site allosterically affects residues distant from the binding site [Jayaraj et al., 2020]. Variations in the apparent K_d depending on the relative concentrations of ligand and the binding protein also have been noted in studies of vitamin D binding to vitamin-D-binding protein. Similar dynamics in conformational ensemble and energetic repartitioning of protein populations have been shown to be functionally important in other physiologic systems, including the tetrameric hemoglobin, which exhibits inter-subunit allostery in oxygen binding [Perutz, 1970; Monod et al., 1965; Koshland et al., 1966; Hilser et al., 2012; Motlagh et al., 2012].

Why would nature create such an allosteric mechanism in binding proteins? Our findings of nonlinear dynamics of estradiol's binding and the allosteric coupling of monomers within SHBG have potential physiological implications. First, the dynamic changes in K_d enabled by the dynamic conformational changes in SHBG upon ligand binding provide a versatile mechanism for extending the range of estradiol binding than would be possible if there were a single fixed K_d . The estradiol concentrations vary widely during different phases of the reproductive and nonreproductive phases of an individual's life extending from 1 to 6 pg/mL early in life and during menopause to ~ 30 to 500 pg/mL during different phases of the normal menstrual cycle to 30,000 to 40,000 pg/mL during pregnancy. Second, the nonlinear dynamics of estradiol's binding and the allosteric coupling offer a potential mechanism for facile regulation of free hormone bioavailability under different physiologic and disease conditions. An example of this facile regulation is observed in men with hyperthyroidism, some of whom develop gynecomastia. Hyperthyroidism is associated with increased levels of SHBG and alterations in the relative ratio of free estradiol to free testosterone concentrations, which has been implicated in the pathophysiology of breast enlargement in some hyperthyroid men [Chopra and Tulchinsky, 1974]. Similar non-linear processes have been found in other biological systems; we speculate that this may be a more general mechanism in nature to regulate the bioavailability of nutrients and hormones. For instance, at a low partial pressure of oxygen, a relatively greater fraction of oxygen remains unbound to hemoglobin, whereas at higher partial pressures of oxygen, more oxygen becomes bound. We also have found evidence on allostery in testosterone's binding to its various binding sites on human serum albumin [Jayaraj et al., 2021].

Limitations of the study

These findings should be interpreted in the context of the study's limitations. The studies were performed using only estradiol; it is possible that other circulating sex hormones that also bind to the same binding pocket on SHBG, such as testosterone, dihydrotestosterone, and other endogenous as well as exogenous estrogens (e.g., phytoestrogens in diet), might influence the binding of estradiol to SHBG. The studies were performed only in the presence of SHBG; the presence of other binding proteins in human blood, such as human serum albumin and orosomucoid, might affect the binding of estradiol to SHBG. Additional studies are needed to characterize how the presence of other ligands (e.g., testosterone) and binding proteins (e.g., human serum albumin) influences the dynamic binding of estradiol to SHBG. The apparent K_d varies dynamically and non-linearly depending upon the relative concentrations of estradiol and SHBG and may

be influenced further by the presence of other ligands and binding proteins such that the association dynamics cannot be faithfully represented by one or two or even a discrete set of bimolecular association constants. Consequently, any mathematical equation or curve fitting of the allosteric interaction should be constrained by additional structural studies. The binding studies were performed at 37°C using a dialysis buffer that mimicked the ionic composition of human plasma. However, human plasma is a highly complex matrix whose composition likely varies among people; therefore, the apparent K_d values could vary dynamically depending upon the composition of this matrix. Under these diverse physiologic and disease conditions, the nonlinear dynamics of estradiol's binding and the allosteric coupling offer a versatile mechanism for facile regulation of free hormone bioavailability.

In conclusion, we show that estradiol binding to dimeric SHBG is a dynamic, nonlinear process that involves allosteric interaction between the two monomers of SHBG. The binding of estradiol to SHBG induces intramolecular rearrangements in the estradiol-binding pocket of the ligand-occupied monomer as well as in the binding pocket of the second monomer and alters the energy landscape of both monomers. The inter-monomeric allosteric communication is bidirectional—the binding of the second estradiol molecule also impacts the landscape and probability of conformational transitions in the first monomer, which was already bound to estradiol. Allosteric coupling in the SHBG monomers changes the energy landscape such that the two monomers are not equivalent even in the fully bound state. The allosteric interaction in the SHBG dimer may offer a potential mechanism to extend the dynamic binding range and to regulate bioavailability of estradiol, as the estradiol concentrations change several 1000-fold during the various phases of a person's life.

METHODS

All methods can be found in the accompanying [transparent methods supplemental file](#).

Resource availability

Lead contact

Further information and requests for resources and reagents should be directed to and will be fulfilled by contacting Ravi Jasuja (rjasuja@bwh.harvard.edu).

Materials availability

This study did not generate new unique reagents.

Data availability

The experimental equilibrium dialysis and fluorescence data have not been deposited in a public repository but are available from the corresponding author on collaborative basis.

SUPPLEMENTAL INFORMATION

Supplemental information can be found online at <https://doi.org/10.1016/j.isci.2021.102414>.

ACKNOWLEDGMENTS

This work was supported in part by the National Institutes of Health and the National Institute on Aging under grants R43 AG045011 (RJ), R44AG045011 (RJ), 5 P30 AG031679 (SB), 1R15GM129715-01(DLB), and R15 GM128102 (KMT).

AUTHORS CONTRIBUTION

Conceptualization, R.J. and S.B.; Methodology, R.J., D.J.S., A.J., L.P., B.L., B.J., K.M.T., D.L.B., and S.B.; Software, A.J., P.P., and B.L.; Formal Analysis, R.J., D.J.S., A.J., B.L., and S.B.; Investigation, R.J., D.J.S., L.P., and M.K.; Resources, L.P.; Writing—Original Draft, R.J., D.J.S., A.J., and S.B.; Writing—Review & Editing, R.J., D.J.S., P.P., B.J., K.M.T., D.L.B., and S.B.; Visualization, R.J., D.J.S., A.J., and P.P.; Supervision, R.J. and S.B.; Funding Acquisition, R.J. and S.B.

DECLARATION OF INTERESTS

Dr. Jasuja reports receiving NIH grant funding, equity interest in FPT, LLC, and participation in a patent on a method to calculate free sex hormone concentration. These conflicts are overseen by and managed

according to policies of the Office of Industry Interaction of the Mass General Brigham Health Care System. Dr. Bhasin reports receiving research grant funding, unrelated to the research reported in this manuscript, from NIA, NINR, NICHD, AbbVie, Metro International Biotechnology, Alivegen, Transition Therapeutics, and FPT; receiving consultant fees from OPKO; participation in a patent to calculate free sex hormones; and holding equity interest in FPT, LLC. These conflicts are overseen by and managed according to policies of the Office of Industry Interaction of the Mass General Brigham Health Care System. The other authors have nothing to disclose.

Received: January 11, 2021

Revised: February 13, 2021

Accepted: April 7, 2021

Published: June 25, 2021

REFERENCES

- Anderson, D. (1974). Sex-hormone-binding globulin. *Clin. Endocrinol.* 3, 69–96.
- Avvakumov, G., Grishkovskaya, I., Muller, Y., and Hammond, G. (2001). Resolution of the human sex hormone-binding globulin dimer interface and evidence for two steroid-binding sites per homodimer. *J. Biol. Chem.* 276, 34453–34457.
- Burke, C.W., and Anderson, D.C. (1972). Sex-hormone-binding globulin is an oestrogen amplifier. *Nature* 240, 38–40.
- Chodera, J.D., and Noe, F. (2014). Markov state models of biomolecular conformational dynamics. *Curr. Opin. Struct. Biol.* 25, 135–144.
- Chopra, I.N., and Tulchinsky, D. (1974). Status of estrogen-androgen balance in hyperthyroid men with graves' disease. *J. Clin. Endocrinol. Metab.* 38, 269–277.
- Dunn, J.F., Nisula, B.C., and Rodbard, D. (1981). Transport of steroid hormones: binding of 21 endogenous steroids to both testosterone-binding globulin and corticosteroid-binding globulin in human plasma. *J. Clin. Endocrinol. Metab.* 53, 58–68.
- Goldman, A.L., Bhasin, S., Wu, F.C., Krishna, M., Matsumoto, A.M., and Jasuja, R. (2017). A reappraisal of testosterone's binding in circulation: physiological and clinical implications. *Endocr. Rev.* 38, 302–324.
- Grishkovskaya, I., Sklenar, G., Avvakumov, G.V., Dales, D., Behlke, J., Hammond, G.L., and Muller, Y.A. (1999). Crystallization of the N-terminal domain of human sex hormone-binding globulin, the major sex steroid carrier in blood. *Acta Crystallogr. D.* 55, 2053–2055.
- Grishkovskaya, I., Avvakumov, G.V., Sklenar, G., Dales, D., Hammond, G.L., and Muller, Y.A. (2000). Crystal structure of human sex hormone-binding globulin: steroid transport by a laminin G-like domain. *EMBO J.* 19, 504–512.
- Grishkovskaya, I., Avvakumov, G., Hammond, G.L., Catalano, M.G., and Muller, Y.A. (2002). Steroid ligands bind human sex hormone-binding globulin in specific orientations and produce distinct changes in protein conformation. *J. Biol. Chem.* 277, 32086–32093.
- Heinrich-Balard, L., Zeinyeh, W., Déchaud, H., Rivory, P., Roux, A., Pugeat, M., and Cohen, R. (2014). Inverse Relationship between hSHBG affinity for testosterone and hSHBG concentration revealed by surface plasmon resonance. *Mol. Cell Endocrinol.* 399, 201–207.
- Hilser, V.J., Wrabl, J.O., and Motlagh, H.N. (2012). Structural and energetic basis of allostery. *Annu. Rev. Biophys.* 41, 585–609.
- Jayaraj, A., Schwanz, H.A., Spencer, D.J., Bhasin, S., Hamilton, J.A., Jayaram, B., Goldman, A.L., Krishna, M., Krishnan, M., Shah, A., et al. (2021). Allosterically coupled multisite binding of testosterone to human serum albumin. *Endocrinology* 162, bqaa199.
- Koshland, D.E., Nemethy, G., and Filmer, D. (1966). Comparison of experimental binding data and theoretical models in proteins containing subunits. *Biochemistry* 5, 365–385.
- Laurent, M.R., and Vanderschueren, D. (2014). Functional effects of sex hormone-binding globulin variants. *Nat. Rev. Endocrinol.* 10, 516–517.
- Laurent, M.R., Hammond, G., Blokland, M., Jardi, F., Antonio, L., Dubois, V., Khalil, R., Sterk, S.S., Gielen, E., Decallonne, B., et al. (2016). Sex hormone-binding globulin regulation of androgen bioactivity in vivo: validation of the free hormone hypothesis. *Sci. Rep.* 6, 35539.
- Manni, A., Pardridge, W.M., Cefalu, W., Nisula, B.C., Bardin, C.W., Santner, S.J., and Santen, R.J. (1985). Bioavailability of albumin-bound testosterone. *J. Clin. Endocrinol. Metab.* 61, 705–710.
- Mazer, N.A. (2009). A novel spreadsheet method for calculating the free serum concentrations of testosterone, dihydrotestosterone, estradiol, estrone, and cortisol: with illustrative examples from male and female populations. *Steroids* 74, 512–519.
- Metzger, J., Schnitzbauer, A., Meyer, M., Söder, M., Cuilleron, C.Y., Hautmann, E., Huber, E., and Lupp, P.B. (2003). Binding analysis if 1-alpha- and 17-alpha-Dihydrotestosterone derivatives to homodimeric sex hormone-binding globulin. *Biochem* 42, 13735–13745.
- Moll, G.W., Rosenfield, R.L., and Helke, J.H. (1981). Estradiol-testosterone binding interactions and free plasma estradiol under physiological conditions. *J. Clin. Endocrinol. Metab.* 52, 868–874.
- Monod, J., Wyman, J.C.J., and Changeux, J.P. (1965). On the nature of allosteric transitions: a plausible model. *J. Mol. Biol.* 12, 88–118.
- Motlagh, H.N., Li, J., Thompson, E.B., and Hilser, V.J. (2012). Interplay between allostery and intrinsic disorder in an ensemble. *Biochem. Soc. Trans.* 40, 975–980.
- Murphy, B.E. (1968). Binding of testosterone and estradiol in plasma. *Can J. Biochem.* 46, 299–302.
- Nisula, B.C., and Dunn, J.F. (1979). Measurement of the testosterone binding parameters for both testosterone-estradiol binding globulin and albumin in individual serum samples. *Steroids* 34, 771–791.
- Orwoll, E., Lambert, L.C., Marshall, L.M., Phipps, K., Blank, J., Barrett-Connor, E., Cauley, J., Ensrud, K., and Cummings, S. (2006). Testosterone and estradiol among older men. *J. Clin. Endocrinol. Metab.* 91, 1336–1344.
- Pearlman, W.H., Fong, I.F., and Tou, J.H. (1969). A further study of a testosterone-binding component of human pregnancy plasma. *J. Biol. Chem.* 244, 1373.
- Perutz, M.F. (1970). Stereochemistry of cooperative effects in haemoglobin: haem-haem interaction and the problem of allostery. *Nature* 228, 726–734.
- Peters, T. (1996). All about albumin: biochemistry, genetics, and medical applications (Academic Press).
- Petra, P., Adman, E., Orr, W., Woodcock, K., Groff, C., and Sui, L.M. (2001). Arginine-140 and isoleucine-141 determine the 17β-estradiol binding specificity of the sex-steroid binding protein (SBP, or SHBG) of human plasma. *Protein Sci.* 10, 1811–1821.
- Prinz, J., Keller, B., and Noe, F. (2011). Probing molecular kinetics with Markov models: metastable states, Transition Pathways Spectroscopic Observables. *Phys. Chem. Chem. Phys.* 13, 16912–16927.
- Rosner, W., and Smith, R.N. (1975). Isolation and characterization of the testosterone- estradiol binding globulin from human plasma. Use of a novel affinity column. *Biochemistry* 14, 4813–4820.

Schwantes, C.R., McGibbon, R.T., and Pande, V.S. (2014). Perspective: Markov models for long-timescale biomolecular dynamics. *J. Chem. Phys.* *141*, 090901–090907.

Shukla, D., Hernandez, C.K., Weber, J.K., and Pande, V.S. (2015). Markov state models provide insights into dynamic modulation of protein function. *Acc. Chem. Res.* *48*, 414–422.

Södergard, R., Bäckström, T., Shanbhag, V., and Carstensen, H. (1982). Calculation of free and bound fractions of testosterone and estradiol-17 β to human plasma proteins at body temperature. *J. Steroid Biochem.* *16*, 801–810.

Sui, L.M., Hughes, W., Agnes, J.H., and Pétra, P. (1996). Direct evidence for the localization of the steroid-binding site of the plasma sex steroid-binding protein (SBP or SHBG) at the

interface between the subunits. *Protein Sci.* *5*, 2514–2520.

Thayer, K.M., Lakhani, B., and Beveridge, D.L. (2017). Molecular dynamics-markov state model of protein ligand binding and allostery in CRIB-PDZ: conformational selection and induced fit. *J. Phys. Chem. B.* *8*, 5509–5514.

Tietz, N.W. (1986). *Textbook of Clinical Chemistry* (Saunders).

Vermeulen, A., Verdonck, L., and Kaufman, J.M. (1999). A critical evaluation of simple methods for the estimation of free testosterone in serum. *J. Clin. Endocrinol. Metab.* *84*, 3666–3672.

Vigersky, R.A., Kono, S., Sauer, M., Lipsett, M.B., and Loriaux, D.L. (1979). Relative binding of testosterone and estradiol to testosterone-

estradiol-binding globulin. *J. Clin. Endocrinol. Metab.* *49*, 899–904.

Wu, C.H., Motohash, T., Abdel-Rahman, H.A., Flickinger, G.L., and Mikhail, G. (1976). Free and protein-bound plasma estradiol-17 beta during the menstrual cycle. *J. Clin. Endocrinol. Metab.* *43*, 436–445.

Zakharov, M.N., Bhasin, S., Travison, T.G., Xue, R., Ulloor, J., Vasan, R.S., Carter, E.C., Wu, F., and Jasuja, R. (2015). A multi-step, dynamic allosteric model of testosterone's binding to sex hormone binding globulin. *Mol. Cell. Endocrinol.* *399*, 190–200.

Zeginiadou, T., Kolia, S., Kouretas, D., and Antonoglou, O. (1997). Nonlinear binding of sex steroids to albumin and sex hormone binding globulin. *Eur. J. Drug Metab. Pharmacokinet.* *22*, 229–235.

Supplemental information

**Estradiol induces allosteric coupling
and partitioning of sex-hormone-binding
globulin monomers among conformational states**

Ravi Jasuja, Daniel Spencer, Abhilash Jayaraj, Liming Peng, Meenakshi Krishna, Brian Lawney, Priyank Patel, Bhyravabhotla Jayaram, Kelly M. Thayer, David L. Beveridge, and Shalender Bhasin

Transparent Methods

2.1 Equilibrium dialysis measurements

Purified SHBG (human) was obtained from The Binding Site (product code BH089.X, The Binding Site, San Diego, CA). It was characterized for purity on denaturing and non-denaturing gels where it migrated as a monomer and a dimer respectively. We have previously shown that it binds to testosterone with high affinity [Zakharov et al., 2011]. SHBG concentrations in the stock solutions were measured using a Nanodrop ND-1000 Spectrophotometer (ThermoFisher Scientific, Waltham, MA). Absorption was read at 278 nm, the path length was 1 cm, and an extinction coefficient of $56740 \text{ M}^{-1} \text{ cm}^{-1}$ was used [Gasteiger et al., 2005].

The dialysis buffer composition simulated the ionic strength conditions in the blood: 90 mM NaCl, 3 mM KCl, 1.3 mM KH_2PO_4 , 1.9 mM $\text{CaCl}_2 \cdot 2\text{H}_2\text{O}$, 1.1 mM $\text{MgSO}_4 \cdot 7\text{H}_2\text{O}$, 5 mM urea, 23 mM HEPES sodium salt, 30 mM HEPES acid, 8 mM sodium azide, and 1 mL of 0.06% DL lactic acid. Equilibrium dialysis was performed in 96-well plates (Harvard Apparatus, Holliston, MA) with semi-permeable 10 kDa membranes. 200 μL of dialysis buffer was added to the "buffer side", and estradiol and SHBG were added to the "sample side" in a total volume of 200 μL . Dialysis plates were incubated for 24 hours at 37°C , after which 150 μL aliquots were removed from each side for estradiol measurement using a validated LC-MS/MS assay that is certified by the Center for Disease Control's Hormone Standardization Program (HoST) [Snyder et al., 2016; Jasuja et al., 2013]. The lower limit of quantitation of the estradiol LC-MS/MS assay is $1 \text{ pg} \cdot \text{mL}^{-1}$, the linear range extends from 1 to 500 pg/mL , and the intra- and inter-assay coefficients of variation are less than 10%.

2.2 Fluorescence spectroscopy experiments to examine estradiol-induced perturbations in SHBG

Fluorescence spectroscopy studies were performed using a K2 Multifrequency Phase Fluorometer (ISS, Champaign, IL) in 5 mm x 10 mm quartz cuvettes (Starna Cells, Atascadero, CA). Steady-state measurements were performed using an ISS lamp (model 90513) with the current set to 20 A and a photomultiplier tube (PMT) voltage set to 6.5 V. The excitation wavelength was set to 290 nm with a light-path slit width of 2 mm. To correct for Wood's anomaly, a polarizer oriented at 0° was placed in the emission path. Inner filter effects were negligible for the concentrations used. The emission wavelength range was scanned from 314 to 400 nm with a 2 nm step size.

Bis-ANS (4,4'-bis(1-anilinonaphthalene 8-sulfonate, dipotassium Salt, Sigma Aldrich, St. Louis, MO) was used as an extrinsic probe [Zakharov et al., 2011; Farris et al., 1978] in fluorescence lifetime experiments. The solid powder was initially reconstituted in PBS to a concentration of 3.2 mM [Zakharov et al., 2011] (extinction coefficient $16,790 \text{ cm}^2 \cdot \text{mmol}^{-1}$ at 385 nm [Farris et al., 1978]) and stored at room temperature away from light. This parent stock was diluted with PBS to a working stock concentration used for each experiment. For lifetime measurements, the same ISS K2 Multifrequency Phase Fluorometer was used, but the excitation source was a 370 nm light-emitting diode (LED) to excite bis-ANS. Emission of bis-ANS was observed through a 420 nm long-pass filter (Newport Corporation, Irvine, CA). In the multifrequency phase and modulation technique, the intensity of the excitation light is modulated from 10 to 160 MHz (with a total of 10 points), the phase shift and relative modulation of the emitted light (with respect to the excitation) are determined, and the lifetimes are found using well-established equations [Jameson et al., 1984; Ross et al., 2008; Spencer et al., 1969]. The phase and modulation were analyzed as a sum of exponentials using a nonlinear least squares procedure implemented using ISS Vinci software and the goodness of fit to the data of a specific model was assessed using the value of the reduced chi-squared.

2.3 Molecular dynamics studies

Structure of SHBG complexed with estradiol was retrieved from the Research Collaboratory for Structural Bioinformatics (RCSB-PDB ID: 1LHU, Uniprot ID: P04278) [Grishkovskaya et al., 2002a; UniProt, 2017]. The crystallographic water was removed, and hydrogens were added to the structure. Amino acids were then analyzed for correct protonation states using the H++ server [Gordon et al., 2005]. The processed structure was used to make apo, singly bound, and doubly bound SHBG dimers.

Subsequently, each complex was parameterized with a ff14SB force field [Maier et al., 2015] and solvated using TIP3P [Jorgensen et al., 1982] water molecules, where a minimum distance of 10 Å was kept between the solute atoms and box boundary and the electroneutrality of the solvated complex was achieved by adding Na⁺ ions. Periodic boundary conditions were applied along with PME summation [Berendsen et al., 1984] for non-bonded calculations (with a 10 Å cut-off [Ryckaert et al., 1977]), while SHAKE was applied to covalently bonded hydrogen atoms with a 2-fs time step. To achieve a constant pressure environment, a Berenson thermostat was implemented. Each solvated complex was energy-minimized in steps with decreasing force on protein residues and the final, unrestricted minimization was carried out in 1000 steps of steepest descent followed by 2000 steps of conjugate gradient. The complex was then heated to 300 K and maintained by Langevin thermostat [Wu and Brooks, 2003] and fixed with a restraint force of 25 kcal·mol⁻¹·Å⁻². The system was equilibrated by slowly decreasing the restraint force on the complex from the initial 25 kcal·mol⁻¹·Å⁻² to 0.1 kcal·mol⁻¹·Å⁻² and the resulting structure was further equilibrated for 20 ns at 300 K with no restraining force. Thermodynamic parameters were observed for stability and fluctuations, with the production run being carried out in NPT conditions for 5 μs. Complex preparation and MD simulations were performed using the AMBER v. 18 suite of programs [Case et al., 2018] and run on CUDA-enabled Nvidia GPUs employing pmemd [Götz et al., 2012; Salomon-Ferrer et al., 2013] implementation. Analysis was done using custom Python scripts and a module of AMBER [Götz

et al., 2012; Roe and Cheatham, 2013] while structural and data visualization employed VMD and PyMOL [DeLano, 2002].

2.4 Markov State Model construction from clustering and network analysis.

Markov state models were constructed by clustering SHBG trajectories into sub-states based on the root mean square deviation (RMSD). All trajectories (apo, singly bound, and doubly-bound SHBG) were stripped of solvent, ions, and estradiol and were concatenated into a single trajectory to be used as input for clustering. AMBER implementation of k-means clustering was utilized. The trajectory was partitioned into 2 to 12 clusters and used for analyses of sub-states. The population of each sub-state and rate of its conversion to other sub-states was studied using different modules available in AMBER and custom scripts. The states and rate of conversion between states were generated using Python scripts.

STAR Methods:

Lead Contact: Further information and requests for resources and reagents should be directed to and will be fulfilled by contacting Ravi Jasuja (rjasuja@bwh.harvard.edu)

Materials Availability: This study did not generate new unique reagents.

Data Availability: The experimental equilibrium dialysis and fluorescence data have not been deposited in a public repository but are available from the corresponding author on collaborative basis.